Astronomy and Computing 42 (2023) 100670

Contents lists available at ScienceDirect

Astronomy and Computing

journal homepage: www.elsevier.com/locate/ascom

Full length article

AlphaTg: GUI application for flux and limb derivatives of UBVRI, Kepler and TESS pass-bands for asteroseismology applications

J. Adassuriya [a,c,*], K. Sellahewa [b], K.P.S.C. Jayaratne [a], S. Ganesh [d]

[a] Astronomy and Space Science Unit, Department of Physics, University of Colombo, Sri Lanka
[b] Department of Physics, University of Sri Jayawardenapura, Sri Lanka
[c] Astronomy Division, Arthur C Clarke Institute, Sri Lanka
[d] Astronomy and Astrophysics Division, Physical Research Laboratory, Ahmedabad, India

ARTICLE INFO

Article history:
Received 8 September 2021
Accepted 12 November 2022
Available online 22 November 2022

Keywords:
Flux derivatives
Limb darkening derivatives
Limb darkening integrals
Asteroseismology
Theoretical amplitudes
SZ Lyn

ABSTRACT

The flux derivatives, limb darkening integrals and limb darkening derivatives have been used in many astronomical applications. Among these applications, the flux and limb darkening derivatives are mandatory parameters in asteroseismology whenever determining the theoretical amplitudes of stellar pulsations. The amplitude ratio method, which compares the observed amplitudes of UBVRI color bands with the theoretical amplitudes is widely used in asteroseismology. The computation of theoretical amplitudes is very complex and time-consuming due to the dependency on several parameters, including flux and limb darkening derivatives. Besides, more theoretical amplitude models are needed to compare with the observations for an ideal conclusion. In addition, the computation of synthetic line profiles in spectroscopy is also used the flux and limb darkening derivatives; therefore, we introduce the AlphaTg code to determine flux and limb darkening derivatives in a single application to minimize the complexity of computation. The facility enables to compute flux derivatives for any effective temperature (T_{eff}) within the range of 3500 K $\leq T_{eff} \leq$ 50000 K and any gravity value within the range of 0.0 $\leq \log(g) \leq$ 5.0 for UBVRI, Kepler and TESS photometric systems. The limb darkening derivatives can be determined for a spherical degree, l = 0, 1, and 2 for linear, quadratic and non-linear limb darkening laws for the effective temperature range of 3500 K $\leq T_{eff} \leq$ 50000 K and gravity range of 1.0 $\leq \log(g) \leq$ 5.0. A case study is also discussed to explain the usage and limitations of the application.

1. Introduction

Asteroseismology is a remarkable way of probing the stellar interior. This technique is entirely depending on the determination of oscillation frequencies and their modes. These modes are initially classified as radial or non-radial and further narrowed down to mode discrimination by assigning the quantum numbers n, l and m. n is related to the number of radial nodes and is called the overtone of the mode; l is the spherical degree of the mode and specifies the number of surface nodes that are present; m is the azimuthal order of the mode, where m specifies how many of the surface nodes are lines of longitude (Aerts et al., 2010). Among the methods of mode identification, the amplitude ratio method (Balona and Evers, 1999; Garrido, 2000; Ulusoy et al., 2013) is widely used for UBVRI pass-band ground-based observations. The observed amplitudes of the oscillation frequencies of a particular star are matched to the theoretical amplitudes, which are computed through a set of stellar models. This process leads to the determination of oscillation modes *(n, l, m)* and hence, through a deep analysis, the stellar parameters can also be determined. In practice, mode identification and determination of global and internal parameters of pulsating stars are simultaneously performed. The amplitude ratios and phase differences of pass-bands are extensively used in mode discrimination of pulsating stars (Balona and Evers, 1999; Dupret et al., 2005; Garrido et al., 1990; Lenz et al., 2008). The amplitudes and phases of the observed oscillation frequencies are theoretically produced in all these analyses. To compute theoretical amplitudes for a model star, the flux derivatives and limb darkening derivatives must be determined for the desired range of effective temperature and gravity (Dupret et al., 2003; Aerts et al., 2010). A detailed description with the computation of partial derivatives and limb darkening derivatives for Stromgren photometric system can be found in Garrido (2000). Garrido (2000) used the ATLAS9 grid and limb darkening coefficients of Watson (1988) for the calculation of partial derivatives and limb darkening derivatives. The model

* Corresponding author at: Astronomy and Space Science Unit, Department of Physics, University of Colombo, Sri Lanka.
E-mail address: janaka@phys.cmb.ac.lk (J. Adassuriya).
URL: https://science.cmb.ac.lk/physics/ (J. Adassuriya).

https://doi.org/10.1016/j.ascom.2022.100670
2213-1337/

fluxes given by the grids of ALTAS (Castelli and Kurucz, 2004; Kurucz, 1993) for effective temperature T_{eff} from 3500 K to 50000 K and log (g) from 0.0 to 5.0 dex for several metallicities (M/H) with the new opacity distribution functions (ODFs) were widely used in the computations of theoretical amplitudes. There are 476 models in each grid (Castelli and Kurucz, 2004) for a metallicity. A pulsating star with unknown effective temperature and gravity, when observed in ground-based (UBVRI) or space-based (TESS, Kepler, CoRoT), should subjected to a rigorous analysis with set of pulsation models to determine the pulsation modes and stellar parameters. Therefore, the process should start with some initial values of effective temperature and gravity to compute the theoretical amplitudes (Fig. 1). The stellar flux models should be computed for appropriate effective temperatures and gravities and make sure to cover the observational error box of T_{eff} and log(g) (Dupret et al., 2003; Aerts et al., 2010). This iterative process is time consuming if the uncertainty is large, i.e. the error box is big which means more models must be included as shown in Fig. 1. Besides, due to the unavailability of a single tool, for step-by-step processing of extracting flux from ATLAS9 grid, the integration and normalization of the flux for UBVRI, Kepler and TESS bands, fitting a least square for the flux and obtain the flux derivatives at any T_{eff} and log (g) is a burden in computation. We experienced this burden in our analysis of Delta Scuti star, SZ Lyn (Adassuriya et al., 2020) and thought for a code to integrate aforementioned steps to minimize the computation time. More often the initial guess is not the ideal model resulting the computation changes to some other range within the observational error range of effective temperature and gravity. Therefore, a substantial set of models, for example in error box 1 in Fig. 1, 45 models should be considered. In addition, the model fluxes of ATLAS9 depend on the parameters, metallicity (M/H), mixing length parameter (α_{MLT}) and microturbulence (ε) velocity. Therefore, if these parameters are uncertain for the considered star the models multiply by factors. In case of higher uncertainty of T_{eff} and log (g) for a particular star, a wide range of T_{eff} and log (g) models should be considered with several other input parameters from ATLAS9 grids to converge models to the observations. Due to the non-availability of a computer code to calculate flux and limb darkening derivatives for any T_{eff} and log (g) limited models of ATLAS9 and limb darkening grids were used in previous investigations. The limited models always result in lower accuracy (Watson, 1988; Garrido, 2000). Additionally, Daszyńska-Daszkiewicz (2007) shows non-smooth derivatives, $\alpha_{\lambda,T}$, calculated from Kurucz models, can produce artificial minima for a dominant mode of FG Vir. Similar results were seen in Garrido (2000) with a large step size of T_{eff} 500 K and log (g) 0.5 resulting in a non-smooth distribution of flux derivatives. This result may be due to the narrow range of T_{eff} and log (g) considered with limited models. Indeed, the computation even for few models multiplied by several band-pass is computationally expensive.

To mitigate the complex computation, European Helio- and Asteroseismology Network (HELAS[1]) has introduced grids of atmospheric parameters and flux derivatives needed to obtain photometric and radial velocity variations for radial and non-radial pulsations. The computations of flux derivatives for temperature steps of 250 K are available in HELAS for Strömgren (uvby), Johnson (UVB) and Geneva (U,B1,B,B2,V1,V,G). These flux derivatives are also in grid format and user has to plot the values and interpolate to get the flux derivatives at the desired T_{eff} and log (g). Furthermore, the HELAS grids provide only UBV bands of Johnson filter system. This is the only available grid of flux

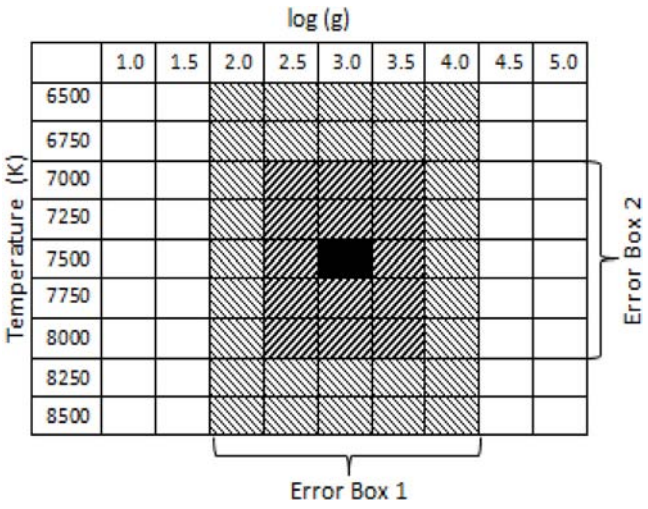

Fig. 1. A representation of Kurucz flux model grid (ATLAS9). The dark square is the target star which may have observational error box either Error Box 1 or Error Box 2 depending on the observation.

derivatives for asteroseismology. In addition to the photometric applications, flux and limb darkening derivatives are also used to produce synthetic line profiles in spectroscopy (Zima, 2006).

Therefore, an application to generate these derivatives for desired T_{eff} and log (g) is timely and important, considering the uprising of model dependent astronomical investigations. We introduce a single code, AlphaTg[2], to lookup tables in ATLAS9 grid to calculate flux derivatives, $\alpha_{\lambda,T}$ and $\alpha_{\lambda,g}$. The same application computes limb darkening integrals ($b_{l,\lambda}$) and hence limb darkening derivatives, $\beta_{\lambda,T}$ and $\beta_{\lambda,g}$ using limb darkening coefficients (hereafter LDC) introduced by Claret and Hauschildt (2003), Claret and Bloemen (2011), Claret (2017). The code includes interactive curve fitting and interpolates the models fluxes and limb darkening integrals and hence computes the flux and limb darkening derivatives for any user-desired value of T_{eff} and log (g) for the Johnson UBVRI, Kepler and TESS pass-bands.

The article is arranged in the following way; In section two, we discuss the dependency of flux and limb darkening derivatives for the computation of theoretical amplitudes for pulsation models. In section three, input parameters, the computation sequences and graphical representation of output parameters are included. Finally, in section four, the observations of SZ Lyn, a Delta Scuti type pulsating star, are used to validate the computations. The possible deviations and limitations are included in the same section. The importance of the facility is highlighted in the conclusions.

2. Theoretical amplitudes

The brightness variations of pulsating stars are the primary parameter to investigate the stellar interior through asteroseismology. These brightness variations are clearly seen in high temporal resolution light curves observed in different pass-bands. The magnitude of this brightness variations can be expressed theoretically using the general expression, Δm_λ, at a wavelength λ for a star;

$$\Delta m_\lambda = A_0 P_{lm}(\cos\ i) b_{l\lambda}(T_1 + T_2 + T_3) e^{j\omega t} \quad (1)$$

where;

$$T_1 = (1 - l)(l + 2)$$

[1] http://helas.astro.uni.wroc.pl/deliverables.php?active=apdescription&lang=en

[2] Download AlpgaTg: https://github.com/kaviphy/AlphaTg/tree/master

$T_2 = f_T(\alpha_{\lambda T} + \beta_{\lambda T})e^{j\psi_T}$

$T_3 = -f_g(\alpha_{\lambda g} + \beta_{\lambda g})$

In Eq. (1), P_{lm} is the associated Legendre function of spherical harmonic degree l and azimuthal number m. A_0 is related to the amplitude of oscillations of the photosphere, i is the inclination angle between the stellar axis and the direction towards the observer and ω is the angular frequency of pulsation. $b_{l\lambda}$ is the limb darkening integral. For the derivations and the details of the components in Eq. (1), refer to Watson (1988), Heynderickx (1994), Balona and Evers (1999), Dupret et al. (2003). The component T_1 is the contribution of the magnitude variation due to the spherical degree l. T_2 and T_3 are the temperature and gravity-dependent component of the magnitude, respectively. The f_T and f_g are amplitudes of temperature and gravity perturbations respectively. The ψ_T is the phase of temperature to the radial displacement of photosphere (Dupret et al., 2003).

2.1. Flux derivatives

The flux of intrinsic variable star changes with changing the temperature and gravity. The perturbation of monochromatic flux at any instant is given by

$$\frac{\delta F_\lambda}{F_{\lambda,0}} = \left[\frac{\partial lnF_\lambda}{\partial lnT_{eff}}\right]\frac{\partial T_{eff}}{T_{eff,0}} + \left[\frac{\partial lnF_\lambda}{\partial lng_e}\right]\frac{\partial g_e}{g_0} \tag{2}$$

$$\alpha_{\lambda T} = \left[\frac{\partial lnF_\lambda}{\partial lnT_{eff}}\right],\ \alpha_{\lambda g} = \left[\frac{\partial lnF_\lambda}{\partial lng_e}\right],$$

$\alpha_{\lambda,T}$ is the partial derivative of flux with respect to temperature at constant gravity. Similarly, $\alpha_{\lambda,g}$ is the partial derivative of flux with respect to gravity at a constant temperature. The theoretical amplitude in Eq. (1) is highly sensitive to $\alpha_{\lambda,T}$ and $\alpha_{\lambda,g}$, hence both are decisive to the determination of theoretical amplitudes of a pulsation model. To determine the accurate flux derivatives of a specific effective temperature and gravity, it is necessary to compute a distribution of flux over the range of temperature and gravity around the best model temperature and gravity of the star (Fig. 1). The derivative depends on the range of the distribution of flux and, in fact, when the range is bigger the distribution is smoother and hence the derivative represents more appropriate value for the flux change. Due to the unavailability of a code to look-up ATLAS9 grids and to include any number of models to compute flux derivatives, the computation is usually limited to the few models close to the initial effective temperature and gravity. To avoid this limitation and improve the accuracy, we introduce our code so that the user desired range of temperature and gravity of the ATLAS9 model grid can be included in the computation. The effect of inclusion of different ranges to the determination of flux derivatives is discussed in Section 4.

2.2. Limb darkening

The intensity of the photosphere of the sun is non-uniform from the center to the limb. This effect is identified as limb darkening. The effect is common to all other stars. Therefore, when the predictions of magnitude variations are required this effect should be included in the computations. The stellar pulsations (Balona and Evers, 1999; Garrido, 2000), determination of planetary parameters using photometric transit method in exo-planet investigations (Csizmadia et al., 2013; Knutson et al., 2007), modeling binary star light-curves (Van Hamme, 1993) and synthetic line profiles in spectroscopy (Zima, 2006) are some of the applications where the limb darkening is extensively used. Linear and non-linear limb darkening laws introduced by Claret (2000), Claret and Hauschildt (2003) are widely used in these applications. The limb darkening integral (Eq. (3)), the linear (Eq. (4)), the quadratic (Eq. (5)) and the non-linear (Eq. (6)) limb darkening laws are defined as

$$b_{l,\lambda} = \int_0^1 \mu I(\mu) P_l(\mu) d\mu \tag{3}$$

$$I(\mu) = 1 - u(1-\mu) \tag{4}$$

$$I(\mu) = 1 - a(1-\mu) - b(1-\mu)^2 \tag{5}$$

$$I(\mu) = 1 - a_1(1-\mu^{1/2}) - a_2(1-\mu) - a_3(1-\mu^{3/2}) - a_4(1-\mu^2) \tag{6}$$

where u, a, b, a_1, a_2, a_3 and a_4 are limb darkening coefficients (LDCs). $P_l(\mu)$ are Legendre polynomials of spherical degree l.

The limb darkening derivatives as a function of effective temperature and gravity are given by

$$\beta_{\lambda T} = \left[\frac{\partial lnb_{l\lambda}}{\partial lnT_{eff}}\right],\ \beta_{\lambda g} = \left[\frac{\partial lnb_{l\lambda}}{\partial lng_e}\right],$$

The LDCs are available as grids for the range of T_{eff}, log (g) and metallicity for pass-bands UBVRI, Kepler and TESS (Claret and Bloemen, 2011; Claret, 2017). Therefore, computation of limb darkening integral in Eq. (3) for set of models and hence determine the limb darkening derivatives ($\beta_{\lambda T}$, $\beta_{\lambda g}$) requires a sequence to look-up LDC tables, integrate limb darkening, curve fitting and determine the derivatives. The code introduced here follows the above sequence of finding LCDs of linear, quadratic and non-linear limb darkening laws for the user input parameters, T_{eff}, log (g) and l. The computations are available for Johnson–Cousins UBVRI, Kepler and TESS pass-bands.

3. AlphaTg code

The AlphaTg is a complete GUI application with two separate menus for flux derivatives and limb darkening derivatives. The entire process of AlphaTg is summarized as a flow chart in Fig. 10. The function of flux derivatives uses ATLAS9 model atmospheres with the options of all chemical abundance (M/H). Claret's limb darkening coefficients are employed for limb darkening derivatives with the options of spherical degree (l) and the three limb darkening laws mentioned in Eqs. (4), (5) and (6). The computations in U, B, V, R, I, Kepler and TESS are separately performed in each menu. After calculating the flux values and limb darkening integrals, the AlphaTg code automatically finds the best least square fit for the data points. The fitted function is used to calculate the flux and limb darkening derivatives for any temperature and gravity values specified by the user.

3.1. Flux derivatives — $\alpha_{\lambda,T}$, $\alpha_{\lambda,g}$

The ATLAS9[3] grid has the options of select parameters, chemical abundance (M/H), turbulence velocity and mixing length for a particular flux model. There are two options in turbulence velocity, 0 km s^{-1} and 2 km s^{-1} and two options for mixing length parameter, 0.5 and 1.25. Due to the fact that models are highly depending on chemical abundance (M/H), all the options of chemical abundance in ATLAS9 grid are included in AlphaTg code as a user selection input. The turbulence velocity is kept constant to its moderate value of 2 km s^{-1}. The mixing length parameter is also kept at 1.25, the highest option in ATLAS9 grid, as recommended in the latest literature in asteroseismology (Bowman and Kurtz, 2018). With these initial user definitions of the models, the

[3] https://wwwuser.oats.inaf.it/castelli/

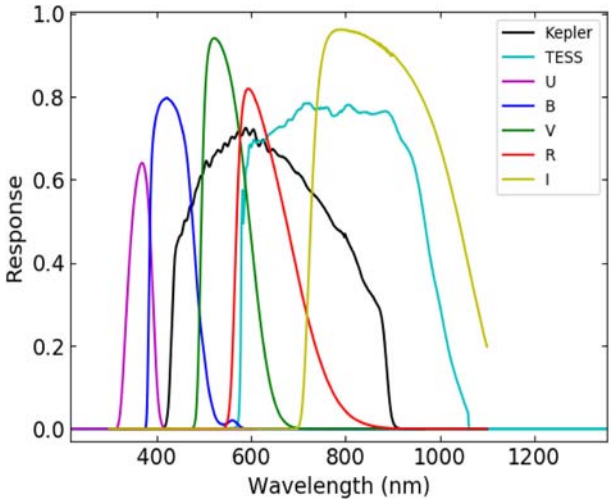

Fig. 2. The response curves of Johnson UBVRI, Kepler and TESS pass-bands.

Table 1
Standard pass-bands used in the accumulation and normalization of the model flux.

Filter	Band-pass (nm)	Central wavelength (nm)
U	300–420	365.6
B	360–560	435.3
V	470–700	547.7
R	550–900	634.9
I	700–920	879.7
Kepler	435–845	640.0[a]
TESS	600–1000	786.5

[a]Van Cleve and Caldwell (2016).

grid offers a data array of temperature from 3500 K to 13000 K in step size of 250 K, 13000 K to 50000 K in step size of 1000 K and gravity, log (g) ranging from 0.0 dex to 5.0 dex in step size of 0.5. The user can select the desired range of temperature and gravity to compute $\alpha_{\lambda,T}$ and $\alpha_{\lambda,g}$ within the entire grid of temperature and gravity available in ATLAS9. For a particular $T_{\rm eff}$ and log (g) model, the flux extends from 10 nm to 10000 nm. The observations in pass-bands do not provide the monochromatic magnitudes. It is rather magnitudes for a particular filter with a transmission curve $\omega_i(\lambda)$ shown in Fig. 2. Therefore, from the entire range of flux of 10 nm to 10000 nm, the flux is measured in the UBVRI, Kepler and TESS pass-bands according to the ranges given in Table 1 (Mitchell et al., 1964; Low and Johnson, 1964; Bessell, 1990). The model flux δF_λ for a pass-band j, is integrated into the filter response range $\lambda_{j,blue}$ to $\lambda_{j,red}$ and given as F_j in Eq. (7).

$$F_j = \int_{\lambda_{j,blue}}^{\lambda_{j,red}} \delta F_\lambda \omega_j(\lambda) d\lambda \tag{7}$$

The pass-band flux values normalized to the filter response are approximated by a higher-order polynomial fit and thus computes the flux derivatives, $\alpha_{\lambda,T}$ and $\alpha_{\lambda,g}$ at any given temperature and gravity. The computed $\alpha_{\lambda,T}$ for the range of 6000 K $\leq T_{\rm eff} \leq$ 9000 K, and $\alpha_{\lambda,g}$ for the range of 1.5 $\leq$ log(g) $\leq$ 5.0 dex are given in Fig. 3 and Fig. 4, respectively.

3.2. Limb darkening derivatives — $\beta_{\lambda,T}$, $\beta_{\lambda,g}$

According to Eq. (3) in Section 2.2, limb darkening depends on spherical degree l and limb darkening laws. In addition to the direct l dependency on magnitude through T_1 (Eq. (1)), the dependency of l on $b_{l,\lambda}$ and hence on limb darkening derivatives

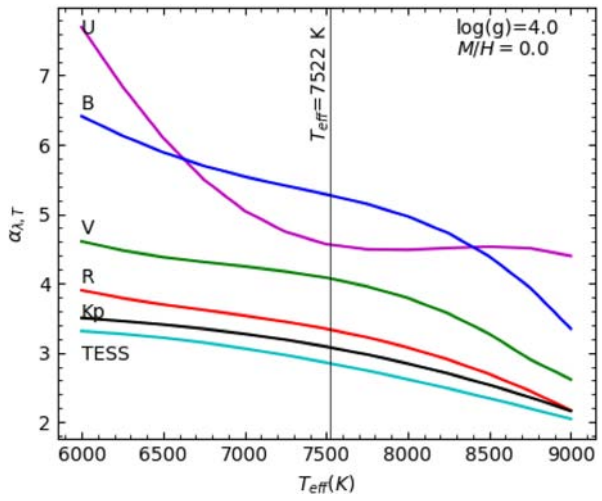

Fig. 3. Flux derivatives $\alpha_{\lambda,T}$ of UBVR, Kepler and TESS bands. The computations were made using ATLAS9 atmospheric models for the range of $T_{\rm eff}$, 6000–9000 K for the constant log (g) = 4.0 and solar chemical abundance of M/H = 0. The vertical line shows the extracted $\alpha_{\lambda,T}$ for the best model of effective temperature to represent SZ Lyn (Adassuriya et al., 2020) (see Section 4).

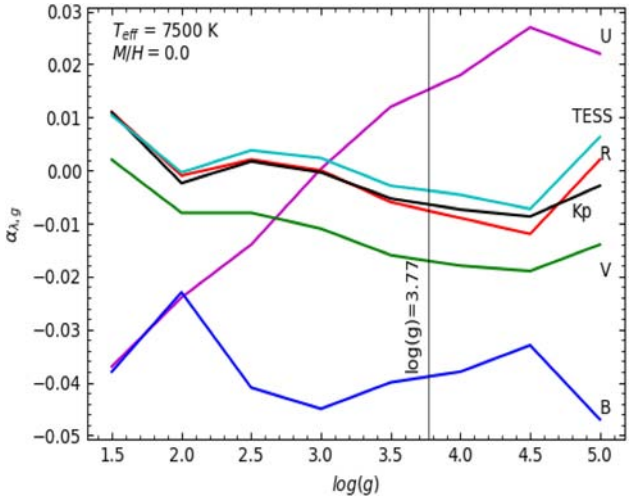

Fig. 4. Flux derivatives $\alpha_{\lambda,g}$ of UBVR, Kepler and TESS bands. The computations were made using ATLAS9 atmospheric models for the range of log (g), 1.5–5.0 dex for the constant $T_{\rm eff}$ = 7500 K and solar chemical abundance of M/H = 0. The vertical line shows the extracted $\alpha_{\lambda,g}$ for the best model of gravity to represent SZ Lyn (Adassuriya et al., 2020) (see Section 4).

$\beta_{\lambda,T}$, $\beta_{\lambda,g}$ in T_2 and T_3 is substantial in amplitude variations. Furthermore, the spherical degree l is the prime parameter to differentiate radial and non-radial modes in asteroseismology. Therefore, the inclusion of $b_{l,\lambda}$, $\beta_{\lambda,T}$ and $\beta_{\lambda,g}$ in theoretical amplitudes and its comparison with an observed amplitude allows us to determine whether the observed pulsation is radial or non-radial. Hence, accurate prediction of both β factors through proper modeling is essential for reliable results in stellar oscillations. One example is briefly discussed in Section 4. We include three options of spherical degree, l = 0, 1, 2, as a user-defined parameter to compute limb darkening derivatives. The higher spherical degree, $l \geq 3$, hardly appears in observed light curve analysis. Therefore, l = 0, 1 and 2 are adequate in any theoretical investigation which supports the observational results. The LDCs of UBVRI[4] (Claret, 2000; Claret and Hauschildt,

[4] http://cdsarc.u-strasbg.fr/viz-bin/qcat?J/A+A/529/A75

Table 2
The available temperature and gravity range for the three limb darkening laws. These limits cause the inconsistent step-sizes and ranges of LDCs of Claret et al. (2012) and Claret (2017) limb darkening grids.

Model	UBVRI	UBVRI	Kepler	Kepler	TESS	TESS
	T_{eff} (K)	log (g) (dex)	T_{eff} (K)	log (g) (dex)	T_{eff} (K)	log (g) (dex)
Linear	5000–10000	1.5–5.0	3500–11750	2.0–5.0	3500–11750	2.0–5.0
Quadratic	2000–9800	3.5–5.0	3500–11750	2.0–5.0	3500–11750	2.0–5.0
Non-Linear	3500–50000	2.0–5.0	3500–11750	2.0–5.0	3500–11750	2.0–5.0

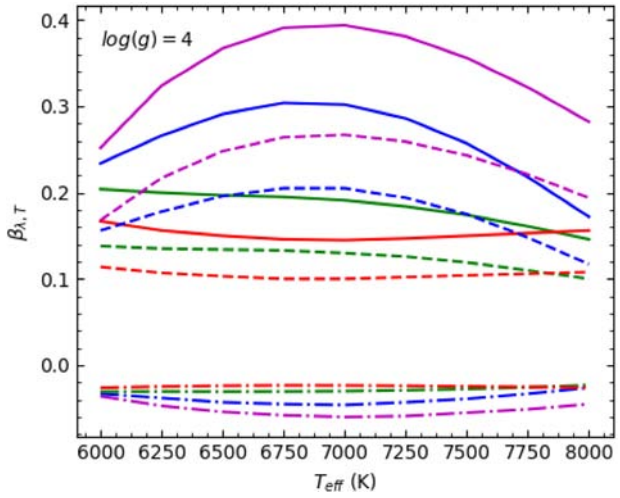

Fig. 5. Limb darkening derivatives of UBVR bands for the range of T_{eff}, 6000–8000 K. The linear limb darkening law for the values of spherical degree, $l = 0$, 1, 2 is used at constant log (g) = 4.0 and solar chemical abundance of M/H = 0. The purple, blue, green and red represent U, B, V and R bands, respectively. The continuous, dashed and dashed–dotted lines represent $l = 0$, $l = 1$ and $l = 2$ respectively.

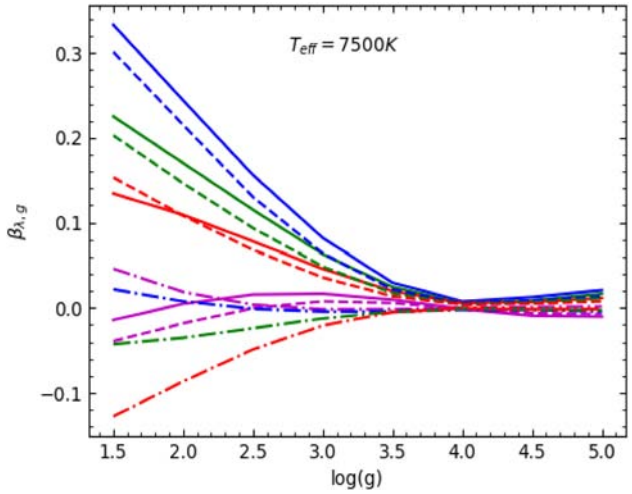

Fig. 6. Limb darkening derivatives of UBVR bands for the range of log (g), 1.5–5.0 dex. The linear limb darkening law for the values of spherical degree, $l = 0$, 1, 2 is used at constant T_{eff} = 7500 K and solar chemical abundance of M/H = 0. The purple, blue, green and red represent U, B, V and R bands, respectively. The continuous, dashed and dashed–dotted lines represent $l = 0$, $l = 1$ and $l = 2$ respectively.

2003), Kepler[5] (Claret et al., 2012) and TESS[6] (Claret, 2017) for the three options, linear, quadratic and non-linear (Eqs. (4)–(6)) are included in AlphaTg. Notice that the LDCs are available for different temperature (T_{eff}) and log (g) ranges in the three limb darkening laws. Table 2 indicates the ranges in which limb darkening integrals and derivatives can be obtained using AlphaTg code. The different temperature and gravity ranges of UBVRI in Table 2 are due to the inconsistent step-size of temperature and gravity of LDCs. The upper limit of 11750 K in Kepler and TESS is also due to the non-availability of LDCs in low gravity range for the $T_{eff} > 11750$ K. For the present purpose, the computed values of linear limb darkening derivatives $\beta_{\lambda,T}$ and $\beta_{\lambda,g}$ of UBVRI are given in Fig. 5 and Fig. 6 respectively. The linear limb darkening derivatives of Kepler and TESS were included in Fig. 7 and Fig. 8. Although the discussion of the variations of these parameters is beyond the scope of this paper, it is obviously seen that $\beta_{\lambda,T}$ is negligible for $l = 2$ and $\beta_{\lambda,g}$ is negligible when log (g) > 3.5, regardless of spherical degree l. The following section includes an application of the code to produce theoretical amplitudes which were analyzed with the observations of a Delta Scuti type short-period pulsating star, SZ Lyn.

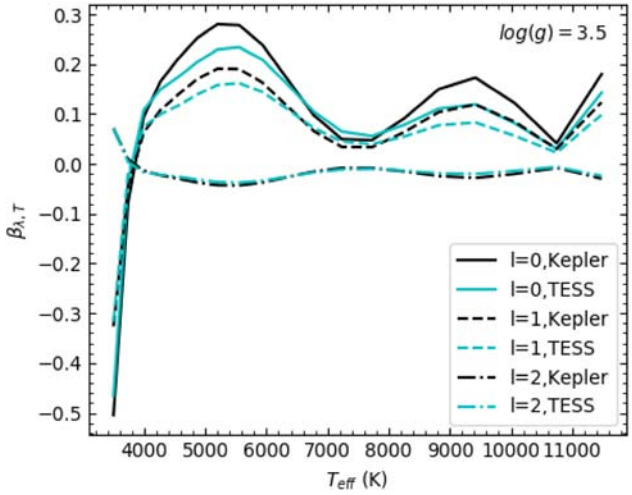

Fig. 7. Limb darkening derivatives of Kepler and TESS pass-bands for the range of T_{eff}, 3500–11750 K. The linear limb darkening law for the values of spherical degree, $l = 0$, 1, 2 is used at constant log (g) = 3.5 and solar chemical abundance of M/H = 0.

4. Case study — SZ Lyn

The computations of flux and limb darkening derivatives produced by AlphaTg were used in a comprehensive astroseismology analysis of SZ Lyn (Adassuriya et al., 2020). SZ Lyn has been observed for its orbital parameters (Moffett et al., 1988; Gazeas et al., 2004; Li and Qian, 2013) as well as physical parameters (Langford, 1976; Fernley et al., 1984). Mode identification of solar-like stars was extensively discussed in Barban et al. (2009), Schofield et al. (2019). The extensive photometric observations in UBVR bands of SZ Lyn, high amplitude Delta Scuti star in a binary system were used for mode identification using amplitude ratio method (Adassuriya et al., 2020). In this analysis, theoretical amplitudes of radial oscillations of SZ Lyn were

5 http://cdsarc.u-strasbg.fr/viz-bin/qcat?J/A+A/529/A75
6 http://cdsarc.u-strasbg.fr/viz-bin/qcat?J/A+A/600/A30

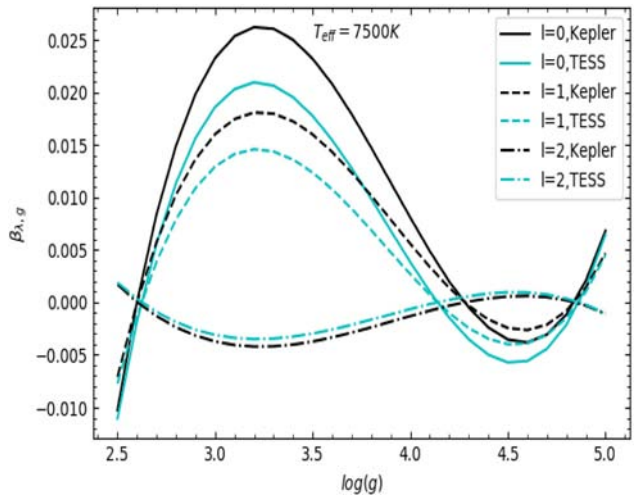

Fig. 8. Limb darkening derivatives of Kepler and TESS pass-bands for the range of log (g), 2.0–5.0 dex. The linear limb darkening law for the values of spherical degree, l = 0, 1, 2 is used at constant T_{eff} = 7500 K and solar chemical abundance of M/H = 0.

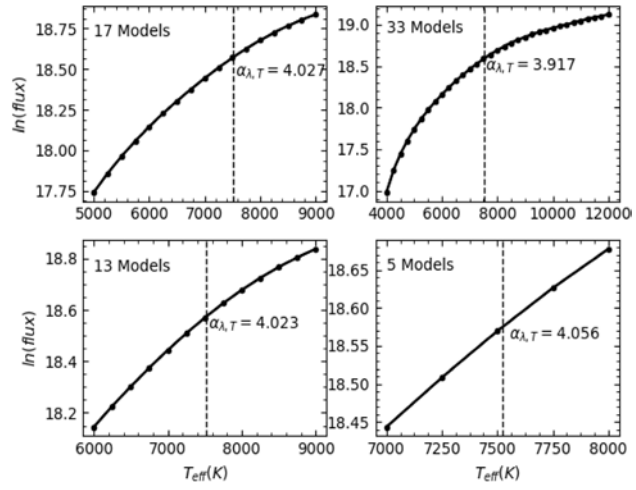

Fig. 9. Four different temperature ranges considered to calculate $\alpha_{\lambda,T}$. The number of models included in the computation is mentioned in each panel. The 9th order polynomial fitting is used to approximate the distribution of flux at each temperature. The $\alpha_{\lambda,T}$ value at T_{eff} = 7522 K which is the best model temperature of SZ Lyn is shown for each range.

computed for several models covering the observational error box. From the previous investigations, SZ Lyn can be initially placed close to the model of T_{eff} = 7500 K and log (g) = 3.5 dex in the ATLAS9 grid. Thus, for the optimization of stellar parameters, the iteration can start from this model and go across this point of T_{eff} and log (g) of the ATLAS9 grid. The user can define a range for T_{eff} and log (g) of ATLAS9 models and here we employ four different ranges of T_{eff} (see Table 3) and log (g) (see Table 4) to evaluate the models with the observations. In the astroseismic analysis of SZ Lyn, the parameters f_T, f_g and ψ_T were generated for several oscillation models using Dupret's non-adiabatic code (Dupret et al., 2003). The best oscillation model which represents SZ Lyn corresponds to T_{eff} = 7522 K and log (g) = 3.77 dex. Therefore computations were initiated from the central model of T_{eff} = 7500 K and log (g) = 3.5 dex in ATLAS9 grid for the calculation of flux derivatives. With the freedom of selecting any range of T_{eff} and log (g) in the ATLAS9 grid, AlphaTg computes flux derivatives, limb darkening integrals and

Table 3
$\alpha_{\lambda,T}$ values calculated for UBVR bands using AlphaTg code for the four different ranges of T_{eff} in ATLAS9 tables. The ranges are selected for the model of T_{eff} = 7522 K log (g) = 3.77 dex of SZ Lyn. The $\alpha_{\lambda,T}$ is exactly taken at T_{eff} = 7522 K (see vertical line in Fig. 3). The Number of models included in the calculation is also given.

T_{eff}	Models	U	B	V	R
7000–8000	5	4.790	5.402	4.056	3.292
6000–9000	13	4.826	5.395	4.023	3.269
5000–9000	17	4.793	5.382	4.027	3.274
4000–12000	33	4.811	5.252	3.917	3.233

Table 4
$\alpha_{\lambda,g}$ values calculated for UBVR bands using AlphaTg code for the four different ranges of log (g) in ATLAS9 tables. The ranges are selected for the model of T_{eff} = 7522 K log (g) = 3.77 of SZ Lyn. $\alpha_{\lambda,g}$ is exactly taken at log(g) = 3.77 dex (see vertical line in Fig. 4).

log(g)	Models	U	B	V	R
1.0–5.0	9	0.015	−0.038	−0.018	−0.008
1.5–5.0	8	0.015	−0.039	−0.018	−0.008
2.0–5.0	7	0.015	−0.039	−0.018	−0.008
2.5–4.5	4	−6.855	−2.122	−0.070	−1.309

limb darkening derivatives across the selected ranges of T_{eff} and log (g) in the ATLAS9 grid and Claret's LDCs. To express the effect of the simplicity of the computation, we have included four ranges of temperature and gravity as shown in Table 3 and Table 4, respectively. The computations of $\alpha_{\lambda,T}$ and $\alpha_{\lambda,g}$ for the best model of SZ Lyn were listed in the same tables. The number of models included in each range is also mentioned. The $\alpha_{\lambda,T}$ and $\alpha_{\lambda,g}$ represent the best model of SZ Lyn are shown as vertical lines in Fig. 3 and Fig. 4 respectively.

From the models of temperature and gravity in both ATLAS9 and LDC grids, the gravity (log (g)), has the lowest number of models. When considering the log (g) in the range from 0.0 to 5.0 with steps of 0.5 dex, the maximum 11 models can be allocated for an analysis. Therefore, the code used 9th order polynomial to fit the flux and limb darkening integrals. The least square fittings of the 9th order polynomial to the synthetic flux for the four ranges of temperature are shown in Fig. 9. The best model of SZ Lyn represents T_{eff} = 7522 K and log (g) = 3.77 dex (Adassuriya et al., 2020). Therefore, using the least square fit, the $\alpha_{\lambda,T}$ and $\alpha_{\lambda,g}$ values were obtained for the above T_{eff} and log (g) and are given in Table 3 and Table 4, respectively. Most importantly, AlphaTg allows to select any range of temperature and thus, calculate the $\alpha_{\lambda,T}$ exactly for the model temperature. Similarly, the range of log (g) can change from 0.0 to 5.0 with steps of 0.5 and therefore, the maximum number of models are limited to 11. However, the number of gravity models are limited depending on the selected effective temperature range. Table 4 shows how $\alpha_{\lambda,g}$ varies with the number of gravity models. Obviously, a very short range of log (g), like 2.5-4.5, not recommended as it would result in unreliable $\alpha_{\lambda,g}$ (see Table 4). Therefore, the full range of log (g) in ATLAS9 grid is recommended for the calculation of $\alpha_{\lambda,g}$. The effect of these ranges in terms of the theoretical and observational amplitudes of SZ Lyn is indicated in Fig. 11.

The overall process AlphaTg is summarized in Fig. 10. The contribution of $\alpha_{\lambda,T}$, $\alpha_{\lambda,g}$, $\beta_{\lambda,T}$ and $\beta_{\lambda,g}$ is indicated in the theoretical amplitude ($A_{\lambda,th}$) in the same diagram. There is a limitation in AlphaTg of interactive curve fitting with a 9th order polynomial for the all distributions. This may be affected for low numbers ($\ll$9) of models and higher numbers of models ($\gg$9) of flux and limb darkening integrals. It can be seen that the fitting may not be perfect with the constant order of polynomial for some temperature ranges, depending on the user's define range. Therefore, a user option is given to output the computed flux and

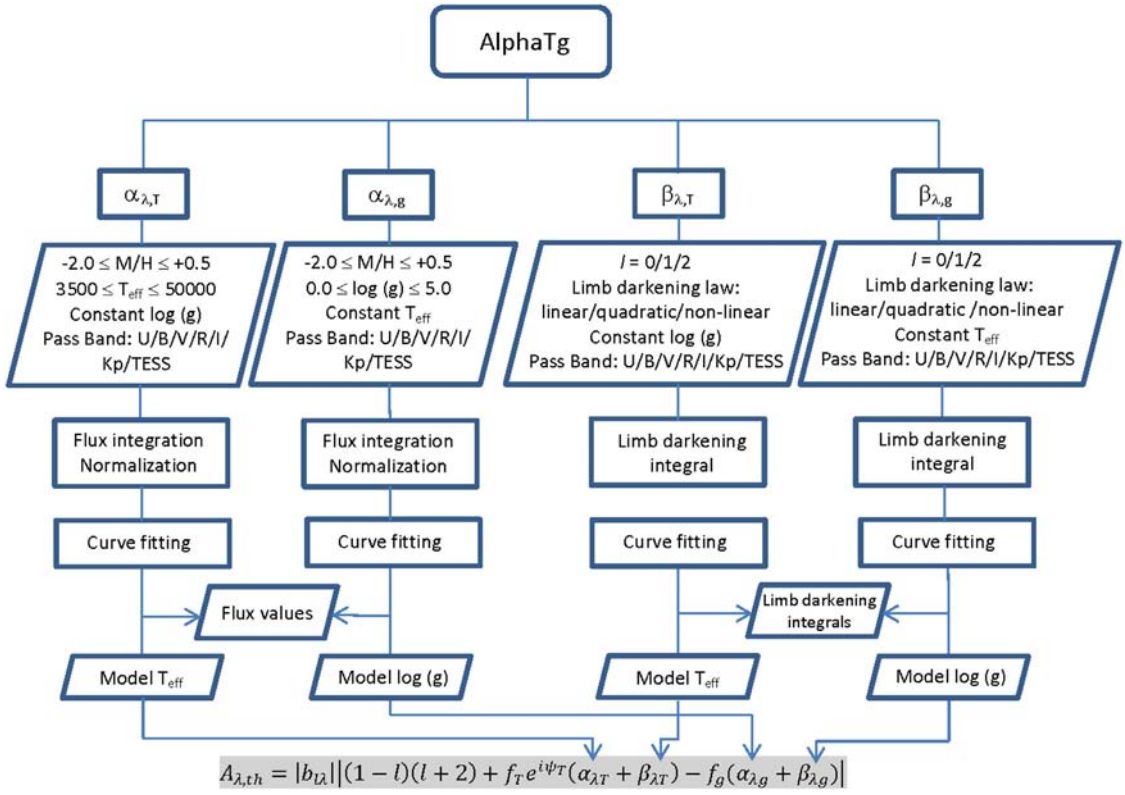

Fig. 10. The flow chart of the entire process.

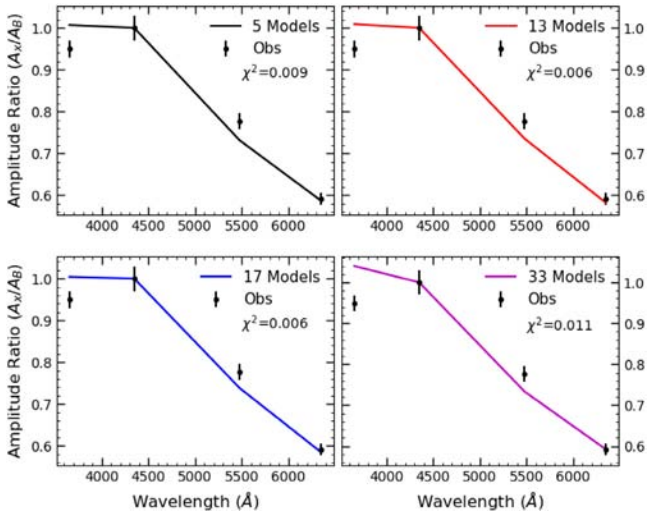

Fig. 11. The comparison of the observed amplitude ratios of SZ Lyn with the theoretical amplitude ratios. The $\alpha_{\lambda,T}$ computed from AlphaTg for different number of models in ATLAS9 grid while The $\alpha_{\lambda,g}$ is calculated for 9 models. The linear limb darkening law for $l = 0$ is used for all limb darkening derivatives. The dots with error bars are the observed amplitude ratios of SZ Lyn. The Chi square is shown for each panel.

limb darkening integrals. This option indicates as an output after the curve fitting process in Fig. 10.

There is a unit discrepancy in the calculated theoretical amplitudes and observed amplitudes in UBVR bands of SZ Lyn. Therefore, theoretical and observed amplitudes could not be brought to a common base-line for comparison. Nevertheless, the theoretical and observational amplitudes can be normalized to a particular pass-band separately (Dupret et al., 2005; Adassuriya et al., 2020). Therefore the theoretical and observational amplitudes of UBVR were normalized to B band and thereafter compared. Fig. 11 shows the comparison of synthetic and observed amplitude ratios for four temperature ranges used to compute $\alpha_{\lambda,T}$. The χ^2 indicates that neither models of higher and lower numbers are appropriate to compute the theoretical amplitudes using AlphaTg. The inclusion of more models, 33 models in Fig. 11 is more deviated from the observation. This may be due to the more flexibility of the interpolation which can be clearly seen in the 33 Models in Fig. 9. Therefore, the inclusion of more number of models away from the initial model may cause higher uncertainty. The least square fitting in Fig. 9 shows how significant the rate of change in flux with the number of models. Therefore, the user has to carefully decide particularly the range of $T_{\rm eff}$ according to the observations. The code provides the facility to analyze different ranges converging the models to observations for an ideal solution. Furthermore, the observations of pulsating stars in UBVRI, Kepler and TESS are encouraged to use the code for flux and limb darkening derivatives to compute synthetic amplitudes for asteroseismology. The effect of stellar rotation is a crucial factor to determine the oscillation modes when the star rotates rapidly. The typical A to F spectral type Delta Scuti stars rotate between 0 and 250 km s^{-1}. Nevertheless, the high amplitude Delta Scuti stars rotate typically $\leq$ 30 km s^{-1} (Breger et al., 1999). Hence, the rotation effect is not included in the case study of high amplitude Delta Scuti star, SZ Lyn. Furthermore, the ATLAS9 flux models and Claret's limb darkening coefficients were defined for non-rotating stars, the flux and limb darkening derivatives produced by AlphaTg are also independent of stellar rotation. We note that the interaction between pulsation and rotation can affect significantly the photometric amplitudes as shown by Daszyńska-Daszkiewicz et al. (2002). Therefore, the rotation effect should be included separately for the outputs of this application specially for the rapidly rotating stars. A comprehensive study of calculation of mode visibilities and amplitude ratios taking into account the

effect of rotation and thereby determine oscillation modes for rapidly spinning stars is discussed in Reese et al. (2009a,b, 2013).

5. Conclusions

We introduced AlphaTg, a GUI for the computation of flux derivatives, $\alpha_{\lambda,T}$, $\alpha_{\lambda,g}$, limb darkening integrals, $b_{l,\lambda}$ and limb darkening derivatives, $\beta_{\lambda,T}$, $\beta_{\lambda,g}$ for mainly asteroseismology and other relevant applications. $\alpha_{\lambda,T}$ and $\alpha_{\lambda,g}$ compute using ATLAS9 model atmospheres and $b_{l,\lambda}$, $\beta_{\lambda,T}$ and $\beta_{\lambda,g}$ compute using limb darkening coefficients. AlphaTg provides flux and limb darkening derivatives for UBVRI, Kepler and TESS pass-bands. The code minimizes rigorous computations process in terms of calculating synthetic amplitudes of oscillating frequencies in asteroseismology.

We showed the usage of the application through the different ranges of T_{eff}, log (g) and limb darkening laws using the case study of SZ Lyn. In this analysis it can be concluded that, even the facility provides to consider different ranges of T_{eff} and log (g), the optimum range should be carefully selected according to the observations and available ranges. It is highly recommended to aware about the ATLAS9 grids and Tables of LDCs before use the AlphaTg. Furthermore, the UBVRI, Kepler and TESS time-series observations of pulsating stars are useful to validate the outputs of the code through the analysis of astroseismology. Nevertheless, the code can be useful to the analysis of UBVRI time-series photometry where the amplitude ratio method is used to identify oscillation modes. In addition, the application is useful to produce purely theoretical amplitudes of oscillation frequencies for a set of different input parameters and hence investigate parameter dependencies.

Declaration of competing interest

The authors declare that they have no known competing financial interests or personal relationships that could have appeared to influence the work reported in this paper.

Data availability

Data will be made available on request.

References

Adassuriya, J., Ganesh, S., Gutiérrez, J., Handler, G., Joshi, S., Jayaratne, K., Baliyan, K., 2020. Asteroseismology of SZ LYN using multi-band high time resolution photometry from ground and space. Mon. Not. R. Astron. Soc..

Aerts, C., Christensen-Dalsgaard, J., Kurtz, D.W., 2010. Asteroseismology. Springer Science & Business Media.

Balona, L., Evers, E., 1999. Mode identification and asteroseismology of δ Scuti stars. Mon. Not. R. Astron. Soc. 302 (2), 349–361.

Barban, C., Deheuvels, S., Baudin, F., Appourchaux, T., Auvergne, M., Ballot, J., Boumier, P., Chaplin, W., García, R., Gaulme, P., et al., 2009. Solar-like oscillations in HD 181420: Data analysis of 156 days of CoRoT data. Astron. Astrophys. 506 (1), 51–56.

Bessell, M., 1990. UBVRI passbands. Publ. Astron. Soc. Pac. 102 (656), 1181.

Bowman, D.M., Kurtz, D.W., 2018. Characterizing the observational properties of δ SCT stars in the era of space photometry from the Kepler mission. Mon. Not. R. Astron. Soc. 476 (3), 3169–3184. doi:10.1093/mnras/sty449.

Breger, M., Pamyatnykh, A., Pikall, H., Garrido, R., 1999. The delta Scuti star FG virginis. IV. Mode identifications and pulsation modelling. Astron. Astrophys. 341, 151–162.

Castelli, F., Kurucz, R., 2004. New grids of ATLAS9 model atmospheres. doi:10.48550/arXiv.astro-ph/0405087, arXiv Preprint Astro-Ph/0405087.

Claret, A., 2000. A new non-linear limb-darkening law for LTE Stellar atmosphere models. Calculations for-5.0<=log [M/H]<=+ 1, 2000 K<=Teff<=50000 K at several surface gravities. Astron. Astrophys. 363, 1081–1190.

Claret, A., 2017. Limb and gravity-darkening coefficients for the TESS satellite at several metallicities, surface gravities, and microturbulent velocities. Astron. Astrophys. 600, A30.

Claret, A., Bloemen, S., 2011. Gravity and limb-darkening coefficients for the Kepler, CoRoT, Spitzer, UVBY, UBVRIJHK, and Sloan photometric systems. Astron. Astrophys. 529, A75.

Claret, A., Hauschildt, P., 2003. The limb-darkening for spherically symmetric NextGen model atmospheres: A–G main-sequence and sub-giant stars. Astron. Astrophys. 412 (1), 241–248.

Claret, A., Hauschildt, P., Witte, S., 2012. New limb-darkening coefficients for PHOENIX/1D model atmospheres-I. Calculations for 1500 K⩽ Teff⩽ 4800 K Kepler, CoRot, Spitzer, UVBY, UBVRIJHK, Sloan, and 2MASS photometric systems. Astron. Astrophys. 546, A14.

Csizmadia, S., Pasternacki, T., Dreyer, C., Cabrera, J., Erikson, A., Rauer, H., 2013. The effect of Stellar limb darkening values on the accuracy of the planet radii derived from photometric transit observations. Astron. Astrophys. 549, A9.

Daszyńska-Daszkiewicz, J., 2007. Approaching asteroseismology of δ Scuti stars: Problems and prospects. doi:10.1553/cia150s32, arXiv Preprint Astro-Ph/0702561.

Daszyńska-Daszkiewicz, J., Dziembowski, W., Pamyatnykh, A., Goupil, M.-J., 2002. Photometric amplitudes and phases of nonradial oscillation in rotating stars. Astron. Astrophys. 392 (1), 151–159.

Dupret, M.-A., De Ridder, J., De Cat, P., Aerts, C., Scuflaire, R., Noels, A., Thoul, A., 2003. A photometric mode identification method, including an improved non-adiabatic treatment of the atmosphere. Astron. Astrophys. 398 (2), 677–685.

Dupret, M.-A., Grigahcene, A., Garrido, R., Gabriel, M., Scuflaire, R., 2005. Convection-pulsation coupling-II. Excitation and stabilization mechanisms in δ SCT and γ DOR stars. Astron. Astrophys. 435 (3), 927–939.

Fernley, J., Jameson, R., Sherrington, M., 1984. BVJHK observations of the dwarf Cepheid SZ Lynx. Mon. Not. R. Astron. Soc. 208 (4), 853–863.

Garrido, R., 2000. Photometric modal discrimination in Delta Scuti and Gamma Doradus stars. arXiv Preprint Astro-Ph/0001064.

Garrido, R., Garcia-Lobo, E., Rodriguez, E., 1990. Modal discrimination of pulsating stars by using Stromgren photometry. Astron. Astrophys. 234, 262–268.

Gazeas, K., Niarchos, P., Boutsia, K., 2004. SZ Lyn: New BVRI CCD observations and improved pulsational and orbital elements. Commun. Asteroseismol. 144, 26–34.

Heynderickx, D., 1994. Geneva seven-colour photometry and frequency analysis of the Delta-Scuti star HD105513. Astron. Astrophys. 283, 835.

Knutson, H.A., Charbonneau, D., Noyes, R.W., Brown, T.M., Gilliland, R.L., 2007. Using Stellar limb-darkening to refine the properties of HD 209458b. Astrophys. J. 655 (1), 564.

Kurucz, R.-L., 1993. ATLAS9 Stellar atmosphere programs and 2km/s grid. Kurucz CD-Rom 13.

Langford, W.R., 1976. Intermediate-Band Photometry of Short Period Dwarf Cepheid Variables (Ph.D. thesis). Brigham Young Univ., Provo, UT..

Lenz, P., Pamyatnykh, A., Breger, M., Antoci, V., 2008. An asteroseismic study of the δ Scuti star 44 Tauri. Astron. Astrophys. 478 (3), 855–863.

Li, L.-J., Qian, S.-B., 2013. Observations and orbital analysis of the high-Amplitude Delta Scuti star SZLyncis: The unusual orbital precession. Publ. Astron. Soc. Japan 65, 116. doi:10.1093/pasj/65.6.116.

Low, F.J., Johnson, H.L., 1964. Stellar photometry at 10 mu. Astrophys. J. 139, 1130.

Mitchell, R., Iriarte, B., Steinmetz, D., Johnson, H., 1964. Photoelectric Photometry of Cepheid Variable Stars. Technical Report, CHICAGO UNIV IL.

Moffett, T.J., Barnes III, T.G., Fekel Jr., F.C., Jefferys, W.H., Achtermann, J.M., 1988. Orbital and photometric properties of SZ Lyncis. Astron. J. 95, 1534–1542.

Reese, D., MacGregor, K., Jackson, S., Skumanich, A., Metcalfe, T., 2009a. Pulsation modes in rapidly rotating Stellar models based on the self-consistent field method. Astron. Astrophys. 506 (1), 189–201.

Reese, D., Prat, V., Barban, C., Van't Veer-Menneret, C., MacGregor, K., 2013. Mode visibilities in rapidly rotating stars. Astron. Astrophys. 550, A77.

Reese, D., Thompson, M., MacGregor, K., Jackson, S., Skumanich, A., Metcalfe, T., 2009b. Mode identification in rapidly rotating stars. Astron. Astrophys. 506 (1), 183–188.

Schofield, M., Chaplin, W.J., Huber, D., Campante, T.L., Davies, G.R., Miglio, A., Ball, W.H., Appourchaux, T., Basu, S., Bedding, T.R., et al., 2019. The asteroseismic target list for solar-like oscillators observed in 2 minute cadence with the transiting exoplanet survey satellite. Astrophys. J. Suppl. Ser. 241 (1), 12.

Ulusoy, C., Gülmez, T., Stateva, I., Dimitrov, D., Iliev, I.K., Kobulnicky, H., Yaşarsoy, B., Alvarez, M., Michel, R., Fox, M.L., et al., 2013. Mode identification in the high-amplitude δ Scuti star V2367 CYG. Mon. Not. R. Astron. Soc. 428 (4), 3551–3558.

Van Cleve, J.E., Caldwell, D.A., 2016. Kepler Instrument Handbook. p. 1, Kepler Science Document KSCI-19033-002.

Van Hamme, W., 1993. New limb-darkening coefficients for modeling binary star light curves. Astron. J. 106, 2096–2117.

Watson, R., 1988. Contributing factors to flux changes in nonradial Stellar pulsations. Astrophys. Space Sci. 140 (2), 255–290.

Zima, W., 2006. A new method for the spectroscopic identification of Stellar non-radial pulsation modes-I. The method and numerical tests. Astron. Astrophys. 455 (1), 227–234.